PHYSICAL REVIEW C

NUCLEAR PHYSICS

THIRD SERIES, VOLUME 24, NUMBER 6 DECEMBER 1981

Ghost anomaly in ^{8}Be studied with ^{9}Be(p,d) at $E_p = 14.3$ and 26.2 MeV

F. D. Becchetti,* C. A. Fields, R. S. Raymond, and H. C. Bhang
Nuclear Physics Laboratory, University of Colorado, Boulder, Colorado 80309

D. Overway
Department of Physics, University of Michigan, Ann Arbor, Michigan 48109
(Received 11 August 1981)

The anomalous feature in ^{8}Be reported at $E_x \approx 0.6$ MeV has been investigated using ^{9}Be$(p,d)^8$Be at 14.3 and 26.2 MeV bombarding energy. Analyses of the spectral shape and transfer cross sections as a function of scattering angle are consistent with this feature being part of the $J^\pi = 0^+$ ^{8}Be g.s. Approximately 6% of the g.s. transfer strength is contained in the anomaly. Also, the line width observed for the $J^\pi = 2^+$ level ($E_x = 2.94$ MeV) appears to be independent of bombarding energy for $E_p = 14$ to 180 MeV.

[NUCLEAR REACTIONS ^{9}Be$(p,d)^8$Be, E_p = 14.3 and 26.2 MeV; measured $\sigma(E_x,\theta)$, $E_x = 0$, 0.6, 2.94, and 11.4 MeV; deduced Γ, γ^2 and S_n; inferred properties of ghost anomaly at $E_x \approx 0.6$ MeV; FRDW analysis; ΔE-E counter telescope and magnetic spectrometer.]

I. INTRODUCTION

An anomalous feature has been observed at an excitation energy of about 0.6 MeV in ^{8}Be in various nuclear reactions.[1-5] This feature has the appearance of a broad level between the $J^\pi = 0^+$ ground state and the wide ($\Gamma \approx 1.5$ MeV) $J^\pi = 2^+$ level at $E_x = 2.94$ MeV (Fig. 1).

This feature has been characterized as a "ghost" of the ^{8}Be g.s. Such an anomaly can rise from an enhancement of the Breit-Wigner tail of a narrow state located near a decay threshold, in this case the ^{8}Be g.s. which is alpha-particle unbound by 92 keV.[6] In this picture the anomalous feature is thus part of the ground state and should exhibit the same quantum numbers, independent of reaction variables.

This explanation for the feature observed in ^{8}Be has been disputed, however,[4,5] since such anomalies can also arise from multibody decay phase-space thresholds.[7,8] Data obtained from low-energy nuclear reactions ($E < 12$ MeV; Refs. 4 and 5), seem to support the latter model, viz., the anomalies observed exhibit angle- and reaction-dependent features which are consistent with phase-space thresholds. These data contain large decay phase-space contributions and it is possible that the ^{8}Be ghost anomaly is obscured. Phase-space contribu-

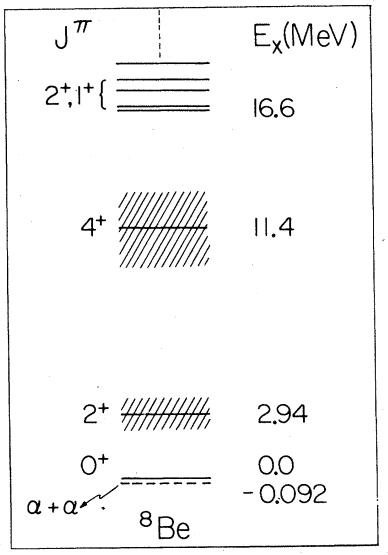

FIG. 1. Level diagram for ^{8}Be (Ref. 6).

tions decrease with increasing bombarding energy, so it is desirable to examine this feature with high-energy reactions. The limited data of this nature which exist[2,3] tend to support the ghost state interpretation. In this paper we present a detailed study of ^{9}Be$(p,d)^8$Be at $E_p=14.3$ and 26.2 MeV. Data were obtained with a ΔE-E Si detector telescope and a high-resolution, low-background magnetic spectrometer system.

II. EXPERIMENTAL PROCEDURES

A. Counter telescope

Data for ^{9}Be(p,d) at $E_p=14.3$ and 26.2 MeV were obtained in a large scattering chamber (100 cm diam.) with a ΔE-E Si counter telescope, consisting of detectors 200 and 5000 μm thick, respectively. These measurements employed a 110 ± 20 μg/cm^2 self-supporting target and yielded data with 60 to 100 keV resolution (FWHM) out to $\theta_{\rm lab}=160°$.

The data obtained with the telescope covered the excitation range $E_x=0-\geq 10$ MeV depending on scattering angle. Spectra are displayed in Figs. 2 and 3.

B. Spectrometer

An energy-analyzed beam of 26.20 ± 0.05 MeV protons was used together with an energy-loss spectrometer ($\Delta\Omega=0.54$ msr) (Ref. 9) for high-resolution spectra. Reaction products were identified in the spectrometer focal plane with a helical delay-line wire proportional co unter backed by a scintillator detector. The latter was used to separate deuterons from other reaction products while the helix counter provided a high-resolution position signal. The detector covered a region of about 10% in ion energy. Beam current was monitored with a water-cooled carbon Faraday cup.

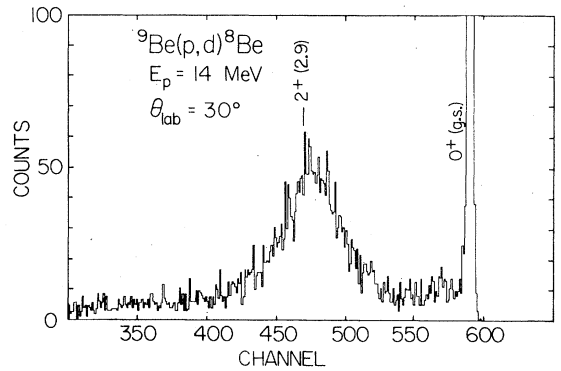

FIG. 2. A ^{9}Be$(p,d)^8$Be spectrum at θ(lab)$=30°$ for $E_p=14.3$ MeV obtained with a Si detector counter telescope. States in ^{8}Be are indicated by J^π and E_x (MeV).

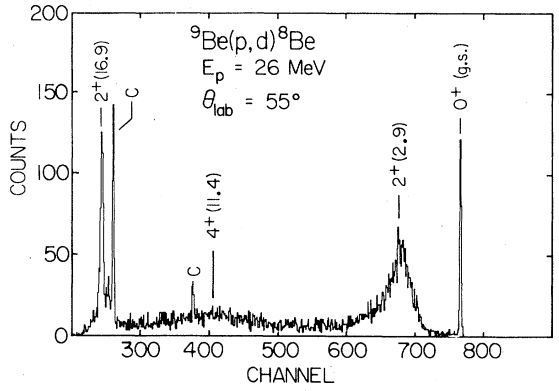

FIG. 3. Same as Fig. 2 for θ (lab) $=$ 55° and $E_p=26.2$ MeV. The groups labeled C are from contaminants in the target.

Reaction products from ^{13}C$(p,d)^{12}$C with a thin target (200 μg/cm^2) were used for position calibration, line-shape, and background measurements. The latter are important as the anomaly observed in ^{8}Be is weak relative to the main g.s. peak. The line shape exhibited little low-energy tailing ($<10^{-3}$ at $E_x\approx1$ MeV) and the background was minimal (see Fig. 4).

Data for ^{9}Be$(p,d)^8$Be were obtained from $\theta=10°-100°$ (lab) with self-supporting ^{9}Be targets, of thicknesses 0.15 and 2.6 mg/cm^2. The thicker target was used for most angles greater than 20°. The resolutions obtained with these targets were about 30 and 70 keV, respectively.

III. DATA

Spectra obtained for ^{9}Be$(p,d)^8$Be are displayed in Figs. 2–5. The solid curves shown in Fig. 5 are theoretical calculations and will be discussed in Sec. IV B.

The anomalous feature in ^{8}Be is clearly observed for $E_p=26.2$ MeV at angles out to θ (lab) $=$ 100° with its maximum at a constant excitation energy (0.6 ± 0.1 MeV). The data were analyzed using semilog plots of the data (Fig. 4), which permitted semiempirical line-shape fits to the peaks at $E_x=0.0$ and $E_x=2.9$ MeV. Contributions from levels $E_x\gtrsim11.4$ MeV are calculated to be small at $E_x\approx0.6$ MeV based on the (p,d) data obtained

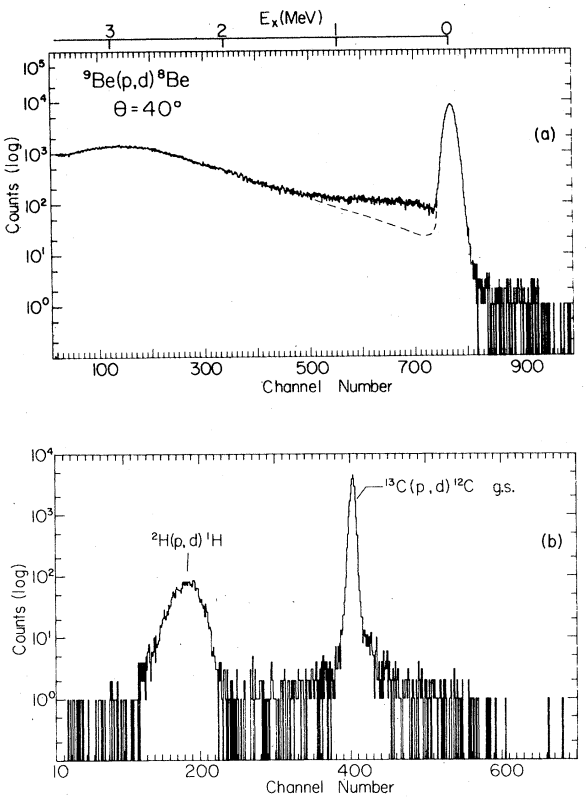

FIG. 4. Top: Data obtained for ^{9}Be(p,d)^{8}Be $E_p = 26.2$ MeV, at $\theta = 40°$ (lab) using a thick target ($\rho x = 2.6$ mg/cm^2). The dashed curves are semiempirical line shapes used to extract cross-section data at $E_x \approx 0.6$ MeV. Bottom: Data from a thin ^{13}C target ($\rho x = 200$ μg/cm^2), $E_p = 26.2$ MeV, $\theta = 10°$ (lab) used to determine the spectrometer line shape and background. The magnetic rigidity (deuteron energy) is about the same as that above.

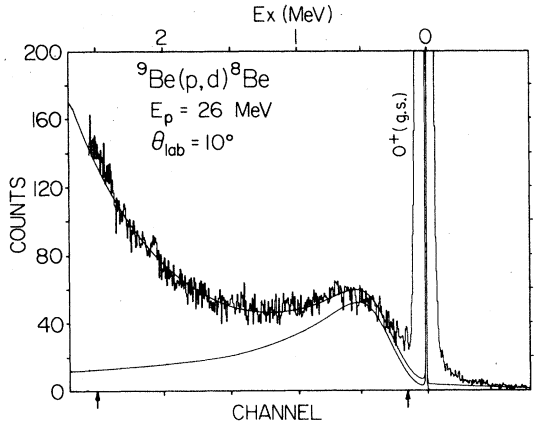

FIG. 5. Spectrum and line-shape fit to thin-target spectrometer data at $\theta = 10°$ (lab). The arrows indicate the region of fit using a two-level formula (see text).

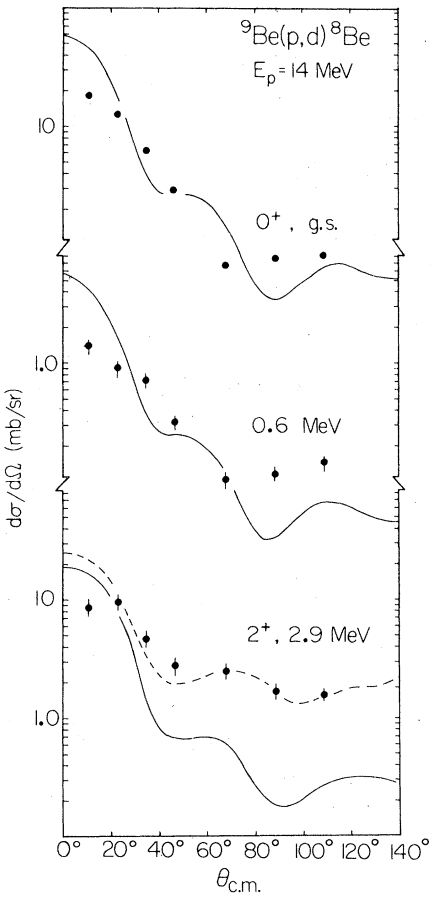

FIG. 6. Cross sections measured at $E_p = 14.3$ MeV. The solid curves are FRDW calculations, while the broken curve is FRDW plus a compound-nuclear contribution (see text).

with the counter telescope (Fig. 3).

The data obtained at $E_p = 14.3$ MeV also exhibit the anomalous feature (Fig. 2) but it is less pronounced due to the poorer energy resolution and greater phase-space contributions. Also, at certain angles protons from the intense ^{9}Be(p,p) elastic events leaked into the deuteron spectrum, obscuring part of the region of interest. It was still possible at most angles to extract cross sections for the anomaly, although with more uncertainties than for $E_p = 26.2$ MeV.

Differential cross sections for the groups observed in ^{8}Be are displayed in Figs. 6 and 7. The curves are theoretical calculations and will be discussed in Sec. IV A. The ratio of cross sections for the group centered at $E_x \approx 0.6$ MeV relative to the

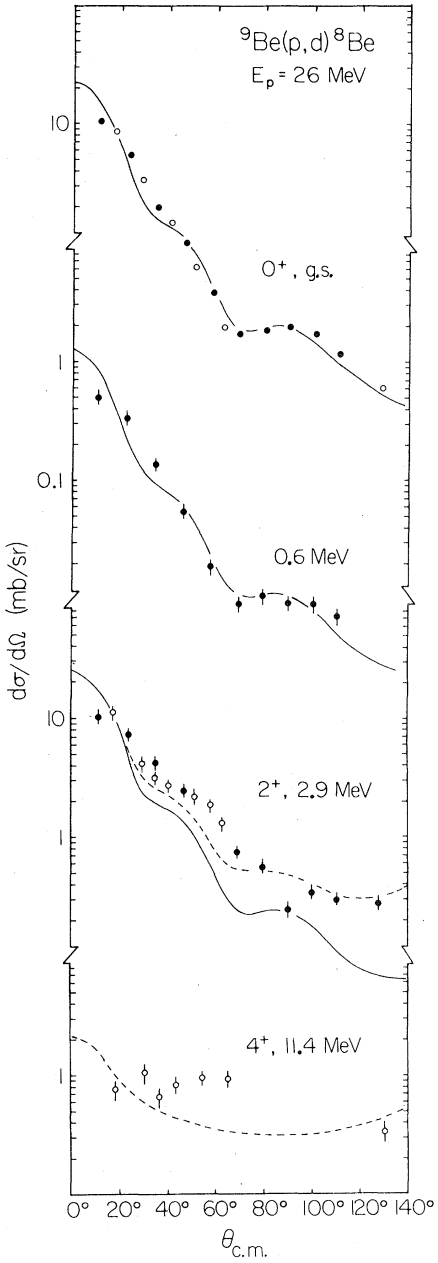

FIG. 7. Cross sections measured at $E_p = 26.2$ MeV. The solid curves are FRDW calculations, while the broken curve includes a compound-nuclear contribution (see text). The open circles are ΔE-E telescope data; the closed circles, spectrometer data.

main g.s. peak is shown in Fig. 8. This ratio is observed to be approximately constant with angle for both $E_p = 14.3$ and 26.2 MeV, although the ratio deduced independently from the counter telescope data is larger by a factor of 2 than that obtained

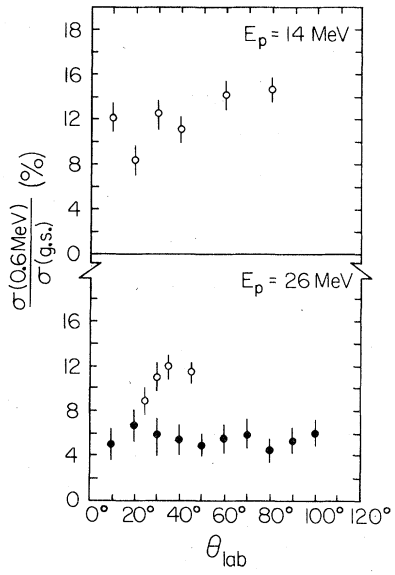

FIG. 8. Ratio of (p,d) cross sections to the anomaly at $E_x \approx 0.6$ MeV relative to the main g.s. peak ($E_x = 0.0$ MeV). The open circles are ΔE-E telescope data (low resolution); the closed circles, spectrometer data (high resolution).

from the high-resolution spectrometer data. We attribute this to differences in the background and resolutions. Our data at $E_x \approx 0.6$ MeV are consistent with the anomaly in ^{8}Be being part of the ^{8}Be g.s., in contrast to the results reported at lower bombarding energies.[4,5] (It appears that the feature observed here at $E_p > 14$ MeV is obscured at lower bombarding energies.) The anomalous feature has also recently been observed with a variety of other reactions.[3]

IV. THEORETICAL CALCULATIONS

A. Angular distributions

Calculations of angular distributions for direct pickup of a $0p_{3/2}$ neutron from ^{9}Be in the (p,d) reaction leading to ^{8}Be ($J^\pi = 0^+$, g.s.) and ^{8}Be ($J^\pi = 2^+$, $E_x = 2.94$ MeV) have been performed using finite-range distorted-wave Born approximation (FRDW).[12] Optical-model parameters from Ref. 13 were employed with neutron bound-state parameters $R = 1.20\,A^{1/3}$ fm, $a = 0.65$ fm and V adjusted to fit the appropriate neutron separation energies.

The resulting calculations, which correspond to a neutron transfer of $l_n = 1\hbar$ from ^{9}Be are shown as

the solid curves in Figs. 6 and 7. Also shown are calculations for the anomaly at $E_x \approx 0.6$ MeV, also assuming $l_n = 1\hbar$ (i.e., $J^\pi = 0^+ or 2^+$). It is apparent that the main 0^+ g.s. component and the group at $E_x \approx 0.6$ MeV are described well by the direct-transfer calculations, especially at $E_p = 26.2$ MeV. The $J^\pi = 2^+$ level exhibits a cross section which falls off more slowly with increasing angle than does the 0^+ g.s. This has been observed in other (p,d) reactions.[10,11] We attribute this to the presence of nondirect, compound-nuclear (CN) deuteron evaporation at large angles, as reported[9] for (p,d) data at $E_p = 33.6$ MeV. The limited data obtained for the $J^\pi = 4^+$ level ($E_x = 11.4$ MeV, Fig. 7) exhibit a relatively flat angular distribution, indicating that this level is probably dominated by a nondirect process, presumably compound nuclear decay. Assuming the data at $\theta > 120°$ arise from CN decay we have calculated CN angular distributions (Fig. 7). Adding these CN cross sections incoherently to the direct-transfer FRDW calculation for the 2^+ level yields the dashed curves shown in Figs. 6 and 7. (Contributions to $J^\pi = 0^+$ levels are about five times smaller.) The addition of a nondirect CN component greatly improves the fits to the $J^\pi = 2^+$ level. It should be noted that at $E_p = 26.2$ MeV the angular distribution of the feature at $E_x \approx 0.6$ MeV is nearly identical to that of the main g.s. peak, and differs from that of the $J^\pi = 2^+$ level. This is consistent with this feature being part of the ^{8}Be g.s. rather than the $J^\pi = 2^+$ level. The angular distributions at $E_p = 14.3$ MeV, although less distinctive, do not contradict this picture (Fig. 6).

The "absolute" neutron spectroscopic factors inferred (Table I) are somewhat larger than other published experimental or theoretical values,[11,14] viz., ^{8}Be (0^+, $E_x = 0.0 + 0.6$ MeV), $S_n = 1.2$ to 1.5. The deduced absolute spectroscopic factors are sensitive to the choice of the FRDW parameters, however, particularly the bound-state parameters. Inclusion of the $E_x \approx 0.6$ MeV anomaly increases the g.s. spectroscopic factor by about 10% relative to that inferred from the main g.s. group.

B. Line-shape analysis

We have performed a least-squares computer fit[15] of several of the spectrometer spectra for the region $E_x \approx 0.2$ to 3 MeV with a two-level spectral distribution of the form[3,8]

$$N(E) \propto \rho(E)[N_{\mathrm{BW}}(E_x = 0.0 \text{ MeV}) + N_{\mathrm{BW}}(E_x = 2.9 \text{ MeV}) + B], \tag{1}$$

where $\rho(E)$ is a phase-space factor[3,7,8] and B is a term (here an exponential, ≈ 0) which represents the background.

The quantities $N_{\mathrm{BW}}(E)$ are Breit-Wigner line-shape forms[3,16]

$$N_{\mathrm{BW}}(E) = A \frac{\Gamma(E)}{(E - E_R)^2 + [\frac{1}{2}\Gamma(E)]^2} \frac{1}{k}, \tag{2}$$

where $\Gamma(E) = 2\gamma^2 P_l(E)$, A is a normalization constant, k is the wave number in the decay channel ($^8\mathrm{Be} \rightarrow \alpha + \alpha$), γ^2 is the reduced α-decay width, E_R is the resonance energy, $[= E_\lambda + \Delta(E)]$, and $\Delta(E)$ is a shift function[3,16]. $P_l(E)$ is a function related to the penetrability for the decay channel. The quantity E_λ is the formal resonance energy.[16]

It is expedient for line-shape analyses to set $\Delta(E)$ = constant (e.g., $=0$) for all E and define the resonance width and energy as $\Gamma_R = \Gamma(E_R) = 2\gamma^2 P_l(E_R)$ and $E_r = E_\lambda$. The quantities Γ_R and E_R are still closely related to the resonance FWHM ($\Gamma_{\mathrm{c.m.}}$) and centroid ($E_{\mathrm{c.m.}}$) but include an appropriate correction for decay penetrabilities. This is required to account for line shapes near decay thresholds.[3]

The formal resonance widths and energy ($\Gamma_\lambda, \gamma_\lambda^2, E_\gamma$), which are determined via Eq. (2) with a shift function appropriate to $P_l(E)$, are very model dependent since $\Delta(E)$ is a function of γ_λ^2. This couples E_λ with Γ_λ and γ_λ^2, resulting in considerable ambiguities in the determination of these quantities.[1,3] Nonetheless, γ_λ^2 is normally the quantity denoted as the reduced decay width. Usually near threshold one has $\Gamma_\lambda > \Gamma_R > \Gamma_{\mathrm{c.m.}}$.

A fit to the ^{9}Be(p,d) data using Eqs. (1) and (2) is shown in Fig. 5. (A fit to the g.s. directly requires convolution with the experimental line width. This has little effect on the spectral shape for $E_x > 0.2$ MeV, however.) The resulting parameters are given in Table I. One observes that with a reasonable choice of reduced α widths, resonance energies, α-penetrability parameters for the $J^\pi = 2^+$ ($E_x = 2.9$ MeV) and $J^\pi = 0^+$ ($E_x = 0.0$ MeV) levels, and normalization factors, the position and magnitude of the anomalous feature observed at $E_x \approx 0.6$ MeV are well reproduced.[3] This feature can thus be ascribed to that part of the Breit-Wigner tail of the 0^+ g.s. which appears in the continuum as the α-decay penetrability increases rapidly to unity.

TABLE I. ^{8}Be levels and spectroscopic factors observed in ^{9}Be(p,d).

J^{π}[a]	E_x[b] (MeV)	$\Gamma_{c.m.}$[c] (MeV)	Γ_R[d]	γ^2[e] (MeV)	l_j[f]	S_{EXP}[g]	S_{CK}[h]
$E_p=14.3$ MeV							
0^+	0.0				$p_{3/2}$	1.13	0.58
(0^+)	0.6				$p_{3/2}$	0.10	
					$p_{1/2}$		0.06
2^+	2.94	1.43(5)	1.6(1)	0.58(5)	$p_{3/2}$	0.22	0.67
					ΣS_n	1.45	1.31
4^+	11.4						
$E_p=26.2$ MeV							
0^+	0.0		5.5(1.3)[i]	0.45(10)	$p^{3/2}$	1.45	0.58
(0^+)	0.6				$p_{3/2}$	0.08	
2^+	2.94	1.51(5)	1.6(1)	0.58(5)	$p_{3/2}$	1.02	0.67
					$p_{1/2}$		0.06
					ΣS_n	2.55	1.31
4^+	11.4	5.2(1)	5.9(1)	0.85(5)			

[a]Spin and parity of ^{8}Be level (Ref. 6). We assume the anomaly observed at $E_x \approx 0.6$ MeV is part of the 0^+ g.s.
[b]Excitation in ^{8}Be (Ref. 6).
[c]The full width at half maximum of the observed resonance in the ^{8}Be c.m. system. The uncertainty in the last digits is indicated in parentheses.
[d]The resonance width defined by Eq. (2) with $\Delta(E)$ set equal to a constant (see Ref. 3). The uncertainty in the last digits is indicated in parentheses. Except as noted, the Γ_R values are in MeV.
[e]The reduced α-decay width inferred from analysis of the line shape using Eq. (2) with the shift function set equal to a constant (see Ref. 3).
[f]The angular momentum quantum numbers assumed for the nucleon picked up from ^{9}Be. Our calculations used $0p_{3/2}$ only but $0p_{1/2}$ would give similar results for the 2^+ level.
[g]Absolute spectroscopic factors inferred from fits to the experimental data (Figs. 6 and 7) using finite-range DWBA assuming unity for the overlap $d \rightarrow p+n$.
[h]Theoretical neutron spectroscopic factors for a pure p^n shell-model calculation [S. Cohen and D. Kurath, Nucl. Phys. A101, 1 (1967)].
[i]Γ_R for the g.s. (in eV) has been inferred from the position and maximum of the ghost anomaly relative to the main g.s. peak, which is assumed to be 92 keV above the α-decay threshold (Ref. 6).

The exact location and magnitude of the anomaly depends sensitively on γ^2 and $P_l(E)$, and thus can provide a measure of the former for a specified penetrability function. If we assume $\Delta(E)$ = constant independent of E or γ^2 [e.g., $\Delta(E)=0$] we obtain the area and position of the ghost anomaly as a function of γ^2 as shown in Fig. 9. (These calculations assume that the main g.s. peak is 92 keV above the $\alpha+\alpha$ threshold, Fig. 1.) The ratio of the area of the ghost anomaly to the main g.s. peak, as determined by the spectrometer data (which is the most precise) indicates $\gamma^2=0.45\pm0.10$ MeV. This is also consistent with $E_x=0.60\pm0.10$ MeV for the maximum of the ghost anomaly, although the latter is primarily determined by the position of the main g.s. peak (i.e., E_R). The γ^2 deduced corresponds to $\Gamma_R=5.5\pm1.3$ eV for the g.s. width. This compares favorably with other measurements[6,17]. Analyses of the $J^{\pi}=2^+$ and 4^+ line shapes are presented in Table I. We note γ^2 (g.s.) $\approx\gamma^2(2^+)\approx\gamma^2(4^+)$ as expected from an α-particle rotational model for ^{8}Be.

Although the values of γ^2 quoted in Table I correspond to a particular choice of shift function,

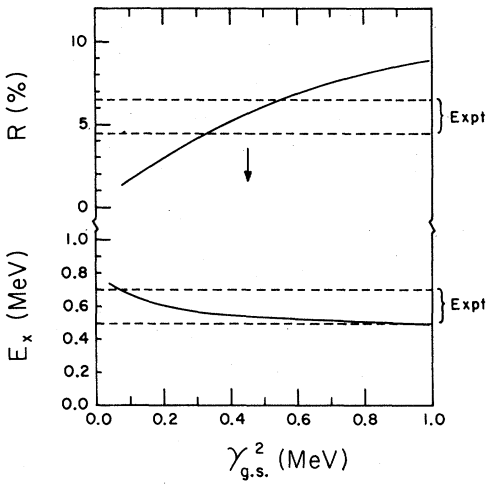

FIG. 9. Top: Ratio of area of ghost peak ($E_x \approx 0.2$ to 1.6 MeV) relative to that of the main g.s. calculated as a function of the reduced g.s. α-decay width. The calculations assume $\Delta(E)$= constant. Bottom: Calculated maximum of the ghost peak as a function of γ^2 (g.s.).

they are typically only 10–20% less than formal values γ_λ^2 obtained using the energy-dependent shift function $\Delta(E)$.

V. BOMBARDING-ENERGY DEPENDENCE OF LINE WIDTHS

The possible reaction-dependence of observed nuclear decay line widths has been the subject of several papers.[2–5] Data for ^{9}Be(p,d) ^{8}Be* now exist[2,3,10,11] over a large energy range (E_p = 8–180 MeV). We have extracted the width $\Gamma_{c.m.}$ for the $J^\pi = 2^+$ (2.9 MeV) level in ^{8}Be from these data. They are displayed in Fig. 10 as a function of bombarding energy. Within the experimental uncertainties little if any dependence on E_p is observed, in agreement with the analysis in Ref. 3.

The reaction dependence of $\Gamma_{c.m.}$ reported in Refs. 5 and 18 can be attributed to the poor-resolution data employed or the lack of self-consistent analysis of $\Gamma_{c.m.}$ between different reactions.

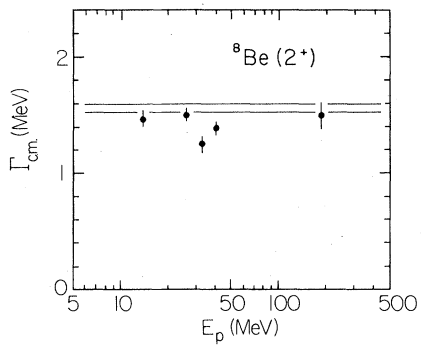

FIG. 10. Measurements of $\Gamma_{c.m.}$ (^{8}Be*, $E_x = 2.94$ MeV) from analyses of the ^{9}Be(p,d) reaction as a function of bombarding energy [$E_p = 14.3$ and 26.2 MeV, this work; $E_p = 33$ MeV, Ref. 3; $E_p = 40$ MeV, Ref. 2 and F. C. Barker (private communication); $E_p = 180$ MeV, Ref. 11]. The lines represent an average of measurements from other reactions (Ref. 3).

VI. CONCLUSIONS

The anomalous feature observed at $E_x \approx 0.6$ MeV in ^{8}Be using the ^{9}Be($p,d,$) reaction at $E_p = 14.3$ and 26.2 MeV exhibits characteristics consistent with this feature being part of the Briet-Wigner tail of the $J^\pi = 0^+$ ^{8}Be g.s. It is possible that such anomalies exist in other nuclei near decay thresholds. This could affect the interpretation of broad features observed in the continuum with high-energy transfer reactions. The line widths observed for ^{9}Be(p,d)^{8}Be* appear to be independent of bombarding energy for E_p = 14–180 MeV.

ACKNOWLEDGMENTS

The authors thank F. Barker and S. Austin for their comments and E. Sugarbaker for his assistnace during the early stages of experiment. The work at the Nuclear Physics Laboratory in Colorado was supported in part by the U.S. Department of Energy. The work of D.O. and F.B. was supported in part by NSF Grant PHY-78-07754.

*On leave from the University of Michigan, Ann Arbor, Michigan 48109.

[1]F. C. Barker and P. B. Treacy, Nucl. Phys. 38, 33 (1962); H. J. Hay *et al.*, Aust. J. Phys. 20, 59 (1967); F. C. Barker, H. J. Hay, and P. B. Treacy, *ibid.* 21, 239 (1968); F. C. Barker, *ibid.* 22, 293 (1969).
[2]F. C. Barker *et al.*, Aust. J. Phys. 29, 245 (1976).
[3]D. Overway *et al.*, Nucl. Phys. A366, 299 (1981).

[4]Th. Lorenz, Z. Naturforsch. 21a, 1196 (1966).
[5]E. H. Berkowitz, G. L. Marolt, A. A. Rollefson, and C. P. Browne, Phys. Rev. C 4, 1564 (1971).
[6]F. Ajzenberg-Selove, Nucl. Phys. A281, 1 (1977); A320, 1 (1979).
[7]G. C. Ohlsen, Nucl. Instrum. Methods 37, 240 (1965).
[8]R. G. Slobodrian, Rep. Prog. Phys. 34, 175 (1971).
[9]B. W. Ridley *et al.*, Nucl. Instrum. Methods 130, 309 (1975).
[10]L. A. Kull, Ph.D. thesis, Michigan State University, 1967; Phys. Rev. 163, 1066 (1967).
[11]O. Sundberg and J. Kallne, Ark. Fys. 39, 323 (1969).
[12]P. D. Kunz (unpublished).
[13]J. E. Monahan, H. T. Fortune, C. M. Vincent, and R. E. Segel, Phys. Rev. C 3, 2092 (1971).
[14]S. E. Darden, G. Murillo, and S. Sen, Nucl. Phys. A266, 29 (1976).
[15]M. Anderson and D. Overway (unpublished).
[16]A. M. Lane and R. Thomas, Rev. Mod. Phys. 30, 257 (1958).
[17]G. Igo, Phys. Rev. 117, 1079 (1960).
[18]D. Bachelier *et al.*, Nucl. Phys. A126, 60 (1969).